Available online at www.sciencedirect.com
ScienceDirect
International Journal of Pharmaceutics 350 (2008) 265–271
INTERNATIONAL JOURNAL OF PHARMACEUTICS
www.elsevier.com/locate/ijpharm

Effect of cyclosporin A on the brain regional distribution of doxorubicin in rats

Yen-Ju Hsieh [a], Chih-Hsien Chang [b], Shu-Pei Huang [a], Chia-Wen Lin [a], Meng-Nan Wang [a], Yu-Tse Wu [a], Yu-Jen Chen [a,c], Tung-Hu Tsai [a,d,*]

[a] *Institute of Traditional Medicine, National Yang-Ming University, Taipei, Taiwan*
[b] *Institute of Nuclear Energy Research, Taoyuan, Taiwan*
[c] *Department of Radiation Oncology, Mackay Memorial Hospital, Taipei, Taiwan*
[d] *Department of Education and Research, Renai Branch, Taipei City Hospital, Taipei, Taiwan*

Received 4 June 2007; received in revised form 29 August 2007; accepted 3 September 2007
Available online 6 September 2007

Abstract

Doxorubicin (DOX) is an anthracycline antibiotic that possesses broad-spectrum antineoplastic activity, and is one of the most important anticancer agents. The purpose of this study was to investigate the effects of cyclosporine A (CsA) on the brain regional distribution of DOX and its liposome DOX formulation (Lipo-Dox). Liquid chromatography with tandem mass spectrometry (LC–MS/MS) was used to measure DOX in rat plasma and in various brain regions (cerebral cortex, hippocampus, striatum, midbrain, cerebellum, and the rest of brain). Good linearity was achieved over the 5–5000 ng/mL range, with coefficients of correlation greater than 0.995. The limit of quantification for doxorubicin was 5 ng/mL. This study was divided into the following four groups: DOX alone, DOX + CsA, Lipo-Dox alone and Lipo-Dox + CsA. After administering DOX (5 mg/kg, i.v.) alone and DOX + CsA (10 mg/kg, i.v.), it was undetectable in various brain regions. When the same dose of Lipo-Dox (5 mg/kg, i.v.) and Lipo-Dox + CsA (10 mg/kg, i.v.) were given individually, the plasma level and the brain regional level of DOX were much greater than those of DOX given alone. These results indicate that Lipo-Dox prolongs the DOX level in plasma and enhances brain distribution of DOX. The disposition of DOX might be regulated by P-glycoprotein.

Keywords: Brain regional distribution; Doxorubicin; P-glycoprotein; Pharmacokinetics

1. Introduction

Doxorubicin is an anthracycline glycoside anticancer drug with a mechanism of impairing DNA synthesis for tumor cell division. It is most commonly used for the treatment of lymphoma, osteosarcoma and other sarcomas, carcinomas, and melanoma (Schwarzbach et al., 2002; Langer et al., 2006; Lind et al., 2007; Lundberg et al., 2007; Smylie et al., 2007). Blood–brain barrier (BBB) acts as an anatomical and transporter barrier notably due to the presence of tight junctions and the ATP-dependent efflux pump P-glycoprotein (P-gp). Many drugs are excluded from entering the brain, as a result of their lack of transport through the BBB or being pumped out by the P-gp. The pharmacological treatment of brain diseases is often complicated by the inability of potent drugs to pass across the BBB, which is formed by the tight endothelial cell junctions of capillaries within the brain.

A liposome is a spherical vesicle with a membrane composed of a phospholipid and cholesterol bilayer. They are usually used for drug delivery due to their unique properties. Currently, most of these liposome formulations are designed to reduce toxicity and to some extent, to increase the accumulation at the target site in a number of clinical applications. Therefore, DOX delivery to the brain is still a challenge for the research groups. Indeed, to circumvent the limited access of DOX into the brain, different approaches using liposomes (Huwyler et al., 1996) or nanoparticles (Gulyaev et al., 1999), peptide-vector strategy using DOX linked to cationic peptides (Rousselle et al., 2000), P-gp modulator (Fenart et al., 1998), or osmotic pressure modification (Neuwelt et al., 1981) have been investigated. Previously,

* Corresponding author at: National Yang-Ming University, 155 Li-Nong Street, Section 2, Taipei 112, Taiwan. Tel.: +886 2 2826 7115; fax: +886 2 2822 5044.
E-mail address: thsai@ym.edu.tw (T.-H. Tsai).

0378-5173/$ – see front matter © 2007 Elsevier B.V. All rights reserved.
doi:10.1016/j.ijpharm.2007.09.002

Ohnishi et al. (1995) and Wang et al. (2006) have reported that the brain distribution of DOX, an antitumoral agent widely used in the treatment of several cancers, is mainly restricted by P-gp on the BBB under normal physiological conditions.

There are many reports regarding the regulation of P-gp and DOX on the brain. To date, there are no detailed descriptions on various brain regional distributions of DOX on the liposome formulation and its effect on the treatment of CsA. We are therefore to develop an LC–MS/MS method to measure the blood and brain regional concentrations and BBB distribution ratio of doxorubicin in rat. In addition, the effect of liposome formulation and interaction with CsA on the enhancement of DOX penetrated BBB will also be investigated. The increasing delivery of drugs in the brain regions by the inhibition of P-gp is potentially less dangerous than other methods of delivering drugs into these brain regions. This study provides a reliable LC–MS/MS analytical method as well as the regional brain distribution of DOX for clinical application.

2. Experimental

2.1. Materials and reagents

Doxorubicin (DOX) and Khellin (internal standard) was purchased from Sigma Chemicals (St. Louis, MO, USA). CsA was purchased from Novartis Pharma AG (Basel, Switzerland). HPLC-grade methanol and acetonitrile were purchased from Tedia Company Inc. (Fairfield, OH, USA). Ammonium acetate and formic acid were purchased from J.T. Baker (Phillipsburgh, NJ, USA). The water used was Milli-Q grade purified from Millipore (Bedford, MA, USA). All other reagents were of analytical grade, which are commercially available.

Lipo-Dox® (Lipo-Dox) was purchased from Taiwan Tung Yang Biopharm (TTY Biopharm Company Ltd., Taipei, Taiwan). The preparation of Lipo-Dox has been previously described (Hong and Tseng, 2001; Chao et al., 2003). Lipo-Dox is a pegylated liposomal doxorubicin (PLD) with a new formulation similar to Doxil® (ALZA Corp., Palo Alto, CA), except that distearoyl-phosphatidylcholine (DSPC) is used instead of hydrogenated soybean phosphatidylcholine (HSPC). Lipo-Dox contains 2 mg/mL of doxorubicin, and 14 μmol/mL phospholipid. Its lipid compositions are DSPC, cholesterol and PEG–DSPE (molar ratio 3:2:0.3). Lipo-Dox is supplied as 10 mL vials containing 20 mg of doxorubicin. The final concentration of liposomes was estimated by the phosphate assay. It contains 14 μmol/mL phospholipids, and it has an average particle size of 104.2 ± 28.3 nm, determined using dynamic laser scattering with a submicron particle analyzer (N4 plus; Beckman coulter Inc.). The particle size of Lipo-Dox is stable for 2 years.

2.2. Animal and drug administration

Adult, male Sprague–Dawley rats (300 ± 20 g body weight) were provided by the Laboratory Animal Center at National Yang-Ming University (Taipei, Taiwan). These animals were specifically pathogen-free and were allowed to adapt in their environmentally controlled quarters (241 ± 1 °C and 12:12 h light–dark cycle). The base diet (Laboratory Rodent Diet no. 5001, PMI Feeds Inc., Richmond, IN, USA) and water were available *ad libitum*.

Six rats were initially anesthetized with pentobarbital (50 mg/kg, i.p.), remained anesthetized throughout the experimental period and the body temperature of rats was maintained at 37 °C with a heating pad. To examine the effect of a typical P-gp inhibitor, CsA, on the brain distribution of DOX, CsA (10 mg/kg, i.v., dissolved in saline) was administered intravenously 10 min before administering DOX (5 mg/kg, i.v.) and Lipo-Dox (5 mg/kg, i.v.). After 30 min injection of DOX, the rats were sacrificed by cardiac puncture and decapitated for regional brain separation. Blood samples and brain regional tissue were collected and removed into heparinized tube. The regional brain was weighed immediately and the blood sample was centrifuged at 6000 rpm for 10 min at 4 °C to collect the upper layer plasma.

2.3. Sample extraction

For liquid–liquid extraction, 50 μL of plasma, 10 μL of internal standard (khellin, 5 ng/mL) and 1 mL of ethyl acetate was added into clean tubes, followed by vortex mixing for 10 min and centrifuging at 10,000 rpm for another 10 min, the upper organic layer was transferred to a new tube and evaporated to dry under a stream of nitrogen. The dried residue was reconstituted with 100 μL of the mobile phase. A 20 μL aliquot of the supernatant was injected into the LC–MS/MS.

The brain was isolated and weighed into the following regions: the cerebral cortex (CX), hippocampus (HP), striatum (ST), midbrain (MB), cerebellum (CB), and the rest of brain (RB). Subsequently, the regional brain tissue was mixed with 50% MeOH (5 mL/g tissue) for homogenization. Brain tissue analyte was centrifuged at 10,000 rpm for 10 min, and the upper layer was transferred to a new tube. The sample preparation was described the same as the previously described liquid–liquid extraction.

2.4. LC–MS/MS

LC–MS/MS analysis was performed using a Waters 2690 chromatography system with a 996 photodiode array detector (PDA) and an autosampler (Bedford, MA, USA) coupled to a Micromass Quattro Ultima tandem quadrupole mass spectrometry (Micromass, Manchester, UK) equipped with an electrospray interface (ESI). The separation was performed on a ZORBAX Extend-C18 column (150 mm × 4.6 mm I.D.; 5 μm, Agilent, Palo Alto, CA, USA) using water–acetonitrile (40:60, v/v) containing 0.01 % formic acid (pH 3.7) at a flow rate of 0.8 mL/min. The mobile phase was filtered through a Millipore 0.45 μm filter. The injection volume was 20 μL. The analyte infusion experiment was performed using a Mode 22 multiple syringe pump (Harvard, Holliston, MA, USA) for MS/MS optimization.

Analyses were performed in the positive ionization mode by multiple reaction monitoring (MRM) and the following precursors to product ion transitions were used: m/z 544 → 361 for DOX and m/z 261.3 → 246.1 for the internal standard. The fol-

lowing parameters were optimized for DOX analysis: capillary voltage of 2.21 kV for positive ionization mode, desolvation gas (nitrogen) heated to 370 °C, and source block temperature of 80 °C. The cone voltage was set to 20 V and the collision energy voltage to 35 eV. The nebuliser and desolvation gas flows were 110 and 550 L/h, respectively. The collision gas was Argon (99.999%, Sanfu Chem., Taipei, Taiwan) with a pressure of 2.11×10^{-3} m bar. Total data were acquired using a dwell time of 0.3 s and inter-channel delay of 0.1 s. All LC–MS/MS data were processed by the MassLynx version 3.5 NT Quattro data acquisition software.

2.5. Method validation

The linearity of the method was evaluated using freshly prepared spiked plasma and brain samples in the concentration range of 5–5000 ng/mL. All calibration curves of DOX were constructed prior to the experiments with correlation values of at least 0.995. The intra- and inter-day variabilities for DOX were assayed (six replicates) at concentrations of 5, 50, 500, 1000 and 5000 ng/mL on the same day and on six sequential days, respectively. The limit of detection was defined by the concentration with a signal-to-noise ratio (SNR) of 3. The limit of quantification (LOQ) is defined as the lowest analyte concentration that can be measured with a stated level of concentration. The accuracy (% bias) was calculated from the nominal mass concentration (C_{nom}) and the mean value of the observed mass concentration (C_{obs}) as follows: (%) bias = $[(C_{obs} - C_{nom})/(C_{nom})] \times 100$. The relative standard deviation (R.S.D.) was calculated from the observed concentrations as follows: % R.S.D. = [standard deviation (S.D.)/C_{obs}] × 100.

The recovery in plasma and brain were evaluated. The DOX stock solution was added to yield final concentrations of 0.05, 0.5 and 5 μg/mL in 50 μL rat plasma and brain tissue. The experiment was repeated three times. Meanwhile, DOX stock solution was diluted with mobile phase. The plasma, brain tissue samples and the diluted solution were processed with the sample preparation method described above. The ratio of peak area [plasma (brain) sample/diluted solution] for DOX was used to calculate the recovery in plasma and brain tissue samples.

3. Results and discussion

3.1. LC–tandem mass spectrometry

The mass spectrum revealed a base peak of DOX at *m/z* 544 corresponding to $[M\text{-}H]^+$ (Fig. 1A); and its fragmentation when collided with reagent gas, the selected product ion *m/z* 361 was shown in Fig. 1B. The mass transition of *m/z* 544 → 361 was used for the quantification of DOX because of its best response. The mass transitions of internal standard were selected as *m/z* 261.3 → 246.1. The analytes were well separated using the present chromatographic conditions. The retention times DOX and internal standard were around 1 and 2 min, respectively, without any peak interference.

3.2. Optimization of sample extraction

The biological samples were tried to extract by different methods including precipitation in methanol, 60% acetonitrile and 10% perchloric acid. However, these simple protein precipitation methods provide a poor recovery for the extraction of

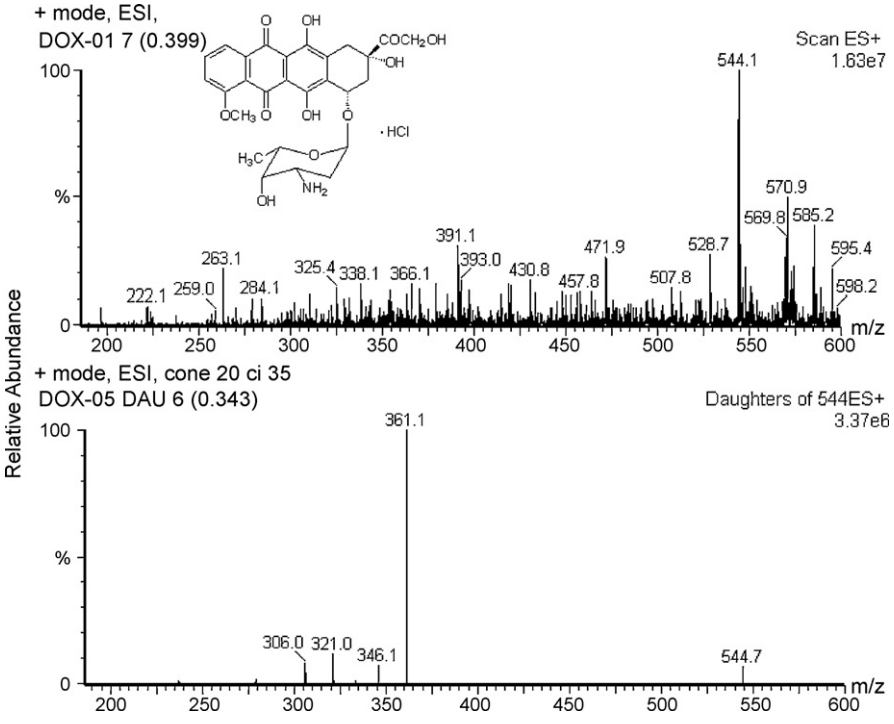

Fig. 1. Full scan mass spectrum (A) and product ion mass spectrum (B) of doxorubicin (molecular weight 543).

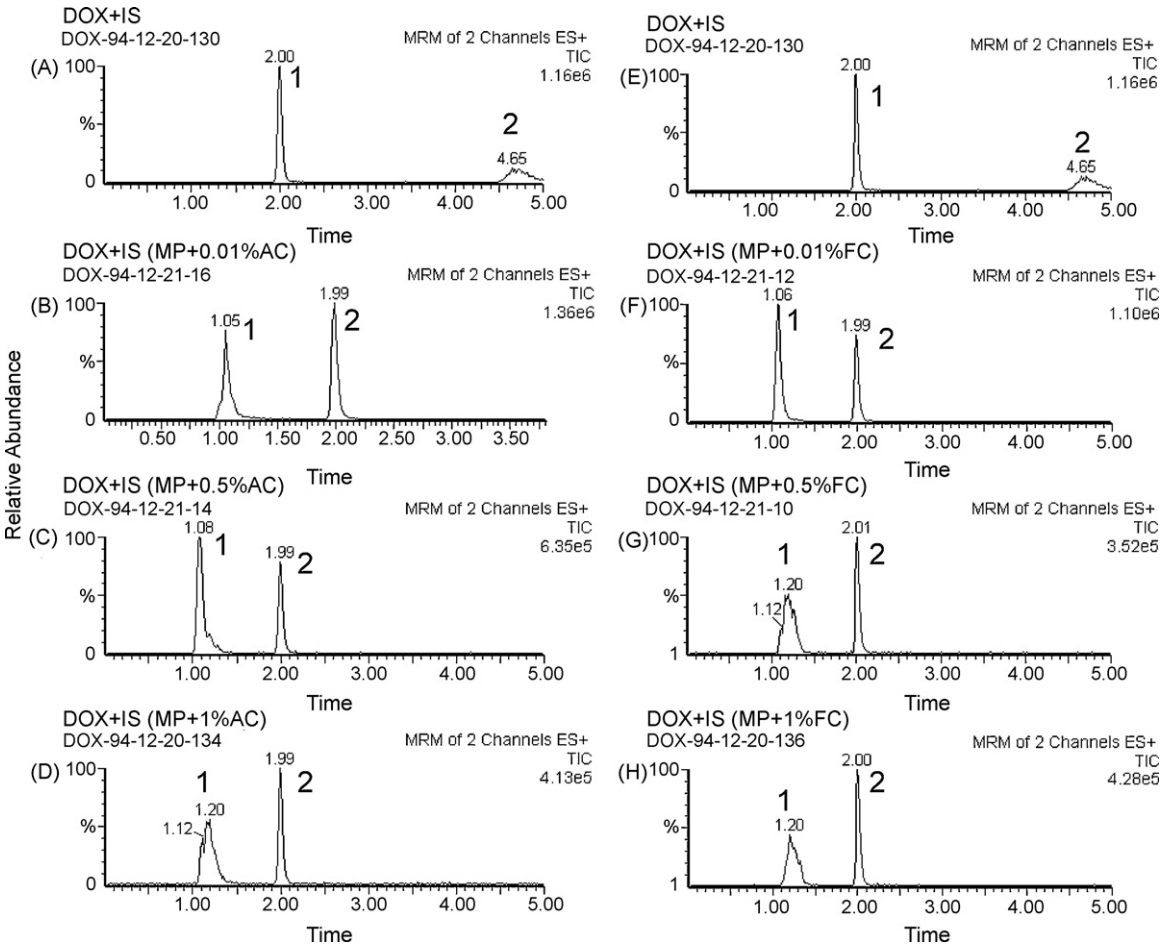

Fig. 2. Effects of concentration of acetic acid and formic acid on the mobile phase of doxorubicin. (A and E) 60% ACN: mobile phase consisting (B) 0.01% acetic acid in 60% ACN, (C) 0.5% acetic acid in 60% ACN, (D) 1% acetic acid in 60% ACN, (F) 0.01% formic acid in 60% ACN, (G) 0.5% formic acid in 60% ACN, and (H) 1% formic acid in 60% ACN. (1): DOX; (2): internal standard.

DOX from plasma and brain samples for LC–MS/MS analysis. This simple protein precipitation procedure was not efficiently applied to extract the analytes from plasma and brain tissue. To improve the recovery, liquid–liquid extraction with ethyl acetate has been used for sample extraction (Cheng et al., 2005). Ethyl acetate has the advantages of high polarity and volatility. The result indicates that DOX recovery in plasma or brain tissue extracted by ethyl acetate was greater than 75 %. Besides, the liquid–liquid extraction procedure was used to avoid the influence of unknown matrix constituents on the analyte signal.

3.3. Optimization of separation

The effects of acetic acid and formic acid concentrations on the resolution of DOX were investigated. Hughes et al. (1998) attempted to separate DOX with the mobile phase of 30% acetonitrile (ACN) and 70% ammonium formate buffer (0.1 M) at pH 4 in a fluorometric detector. Lachatre et al. (2000) also reported that the mixture of 5 mM ammonium formate (pH 3.0)-acetonitrile (70:30, v/v) as the mobile phase for HPLC conditions. It can be seen as the broad and tailing peak of DOX in Fig. 2A–D that the acetic acid concentration ranges of 0, 0.01, 0.5 and 1%, respectively. When the same concentration ranges of formic acid (0, 0.01, 0.5 and 1%) were added (Fig. 2E–H), the data indicate that 0.01% formic acid showed optimal separation and peak shape of DOX and internal standard. The optimized LC–MS/MS conditions were performed isocratically using a mobile phase consisting 0.01 % formic acid in 60% acetonitrile (pH 3.7) separated by C18 column. Under the above conditions, the run time of each sample can be completed within 5 min (Fig. 3).

3.4. Linearity, limit of quantification and detection

The linearity of the calibration graphs was demonstrated by the determination coefficients (r^2) obtained for the regression line. A good linearity was achieved over the 5–5000 ng/mL range, with all coefficients of correlation greater than 0.995. All samples were freshly prepared including the standard solution from the same stock solution (50 μg/mL). The LOD and LOQ were 1 and 5 ng/mL, respectively.

3.5. Precision and accuracy

The intra- and inter-assay precision and accuracy values are presented in Table 1. The overall mean precision, defined by

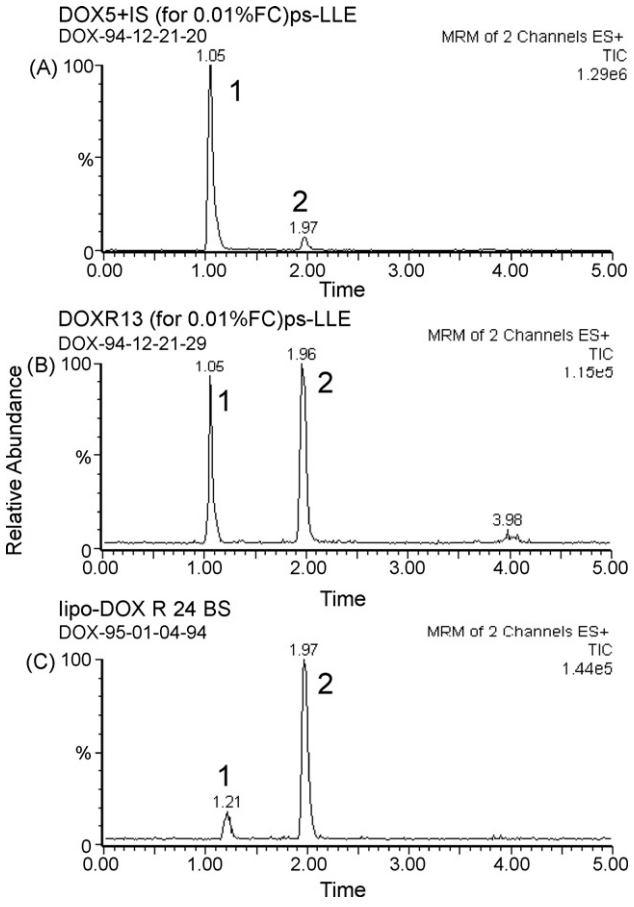

Fig. 3. Chromatograms of (A) standard DOX (RT: 1.05 min) and IS (RT: 1.97 min), (B) blood sample containing DOX collected from the cardiac puncture at 0.5 h after Lipo-Dox administration (5 mg/kg, i.v.), and (C) brain sample containing DOX collected from the decapitation at 0.5 h after Lipo-Dox administration (5 mg/kg, i.v.). (1): DOX; (2): internal standard.

the R.S.D., ranged from 0.08 to 19.5%. Analytical accuracy, expressed as the percent difference of the mean observed values compared with known concentration varied from −0.36 to 12.4%.

Table 1
Intra- and inter-assay accuracy and precision values of the LC–MS/MS method for the determination of doxorubicin in rat plasma

Nominal concentration (ng/mL)	Observed concentration (ng/mL)	Precision (R.S.D.%)	Accuracy (% bias)
Intra-assay ($n=6$)			
5	5.06 ± 0.9	17.7	1.20
50	51.06 ± 5.3	10.3	2.12
500	491.4 ± 24	4.88	−1.72
1000	1015 ± 66	6.50	1.50
5000	4999 ± 26	0.52	−0.02
Inter-assay ($n=6$)			
5	5.62 ± 1.1	19.5	12.4
50	52.18 ± 2.8	5.36	4.36
500	499.7 ± 0.4	0.08	−0.06
1000	1004 ± 58	5.77	0.40
5000	4982 ± 20	0.40	−0.36

Observed mass concentrations are expressed as mean ± S.E.M.

3.6. Plasma level and regional brain distribution

The plasma level of DOX in the treatment of Lipo-Dox (5 mg/kg, i.v.), which was much higher than the DOX (5 mg/kg, i.v.) group untreated with liposomal formulation. CsA partially increased the plasma level of DOX. However, DOX was unable to be detected in both DOX and DOX + CsA groups. Upon treatment with Lipo-Dox (5 mg/kg, i.v.) or the same dose of Lipo-Dox coadministered with CsA (10 mg/kg, i.v.), after 30 min of the drug injection the plasma level of DOX and the brain regional distribution of DOX was significantly increased than those of DOX given alone (Table 2). These results indicate that DOX was unevenly distributed into various brain regions after Lipo-Dox was given. Cerebral cortex and striatum represented the highest and lowest concentration of brain regions, respectively.

Recent reports indicate that the highest DOX concentration was found in the kidney after 30 min of DOX (5 mg/kg, i.v.) administration. Liposomal DOX was significantly higher than DOX alone in the brain distribution of DOX. Coadministered with verapamil (a P-glycoprotein inhibitor) enhances DOX penetrate into brain tissue (Wang et al., 2006), which is consistent with our data. Besides, the brain distribution of DOX was increased twofold when CsA was coadministered with Lipo-Dox, which suggested that the brain transport system of DOX might be regulated by P-glycoprotein.

In this study, the rat brains were removed for analysis without perfusion before sacrifice. During the decapitation, the cerebral pressure forced the blood drain off from the brain that the blood residual should be limited. Compared with the volume of regional brain distribution, the tiny volume of blood residual can be neglected. The same procedure was performed to measure drug level in the regional brain tissue (Hughes et al., 1998; Saito et al., 2001; Zhao et al., 2002; Wang et al., 2006). In

Table 2
Plasma and regional brain concentrations of DOX after 30 min of DOX (5 mg/kg, i.v.) or Lipo-Dox (5 mg/kg, i.v.) in the absence and presence of CsA (10 mg/kg, i.v.) in rats

Drug treatment	Plasma or brain regions	Plasma or regional brain concentration (μg/mL)
DOX	Plasma	0.08 ± 0.008
DOX + CsA	Plasma	0.11 ± 0.021
Lipo-Dox	Plasma	23.2 ± 1.5*
Lipo-Dox + CsA	Plasma	28.6 ± 3.6*
Lipo-Dox	Cerebral cortex	0.12 ± 0.015
Lipo-Dox	Cerebellum	0.22 ± 0.010
Lipo-Dox	Hippocampus	0.06 ± 0.022
Lipo-Dox	Brain stem	0.10 ± 0.005
Lipo-Dox	Striatum	0.008 ± 0.003
Lipo-Dox	The rest of brain	0.13 ± 0.024
Lipo-Dox + CsA	Cerebral cortex	0.22 ± 0.043*
Lipo-Dox + CsA	Cerebellum	0.28 ± 0.023*
Lipo-Dox + CsA	Hippocampus	0.15 ± 0.017*
Lipo-Dox + CsA	Brain stem	0.16 ± 0.025*
Lipo-Dox + CsA	Striatum	0.03 ± 0.010*
Lipo-Dox + CsA	The rest of brain	0.22 ± 0.017*

Data expressed as mean ± S.E., $n=6$. *Significantly different compared with the group of DOX or Lipo-Dox alone ($P<0.05$).

contrast with above method, some experiments perfused brain tissue with physiological solution before sacrifice (Huwyler et al., 1996; Sharma et al., 1997; Arnold et al., 2005). These data shows no significant difference.

Several emitting radionuclides can be used to label liposomes for monitoring the in vivo behavior of liposomes noninvasively. By using imaging systems, such as a gamma camera, the whole body distribution of radiolabeled liposomes in each organ or tissue can be measured at different times in a living animal (Bao et al., 2004; Chen et al., 2007). The radiolabeled Lipo-Dox has been applied in the pharmacokinetics and biodistribution of Lipo-Dox in rodents (Bao et al., 2004). To evaluate the effect of CsA for the uptake of DOX in brain, we also used the radiolabeled liposome. The methods for radiolabeling liposome using Rhenium-188 has been established in our group (Chang et al., 2007; Chen et al., 2007). The project using Indium-111 labeled Lipo-Dox to study the effect of CsA for the uptake of DOX in brain is ongoing. Unpublished data in our laboratory showed that the CsA enhanced the uptake of Lipo-Dox in brain, which is consistent with the results by the LC–MS/MS studies in this manuscript.

4. Conclusions

In conclusion, a sensitive and precise LC–MS/MS was developed to evaluate the regional brain distribution. The data indicate that DOX treated alone could not be able to detect in the brain regions on both the groups of DOX and DOX coadministered with CsA. Upon treating with Lipo-Dox, the DOX can be detected in various brain regions. These results suggest that Lipo-Dox prolongs the DOX level in plasma and enhances DOX penetration in the brain tissue. The brain distribution of DOX was increased twofold when CsA was coadministered with Lipo-Dox, which suggested that the brain transport system of DOX might be regulated by P-glycoprotein.

Acknowledgements

This study was supported in part by research grants (NSC96-2113-M-010-003-MY3; NSC96-2628-B-010-006-MY3 National Science Council, and 96001-62-027 Taipei City Hospital, Taiwan).

References

Arnold, R.D., Mager, D.E., Slack, J.E., Straubinger, R.M., 2005. Effect of repetitive administration of doxorubicin-containing liposomes on plasma pharmacokinetics and drug biodistribution in a rat brain tumor model. Clin. Cancer. Res. 11, 8856–8865.

Bao, A., Goins, B., Klipper, R., Negrete, G., Phillips, W.T., 2004. Direct ^{99m}Tc labeling of pegylated liposomal doxorubicin (Doxil) for pharmacokinetic and non-invasive imaging studies. J. Pharmacol. Exp. Ther. 308, 419–425.

Chang, Y.J., Chang, C.H., Chang, T.J., Yu, C.Y., Chen, L.C., Jan, M.L., Luo, T.Y., Lee, T.W., Ting, G., 2007. Biodistribution, pharmacokinetics and microSPECT/CT imaging of ^{188}Re-BMEDA-liposome in a C26 murine colon carcinoma solid tumor animal model. Anticancer Res. 27, 2217–2225.

Chao, T.C., Wang, W.S., Yen, C.C., Chiou, T.J., Liu, J.H., Chen, P.M., 2003. A dose-escalating pilot study of sterically stabilized, pegylated liposomal doxorubicin (Lipo-Dox) in patients with metastatic breast cancer. Cancer Invest. 21, 837–847.

Chen, L.C., Chang, C.H., Yu, C.Y., Chang, Y.J., Hsu, W.C., Ho, C.L., Yeh, C.H., Luo, T.Y., Lee, T.W., Ting, G., 2007. Biodistribution, pharmacokinetics and imaging of ^{188}Re-BMEDA-labeled pegylated liposomes after intraperitoneal injection in a C26 colon carcinoma ascites mouse model. Nucl. Med. Biol. 34, 415–423.

Cheng, C.L., Chou, C.H., Hu, O.Y., 2005. Determination of lamotrigine in small volumes of plasma by high-performance liquid chromatography. J. Chromatogr. B 817, 199–206.

Fenart, L., Buee-Scherrer, V., Descamps, L., Duhem, C., Poullain, M.G., Cecchelli, R., Dehouck, M.P., 1998. Inhibition of P-glycoprotein: rapid assessment of its implication in blood–brain barrier integrity and drug transport to the brain by an in vitro model of the blood–brain barrier. Pharm. Res. 15, 993–1000.

Gulyaev, A.E., Gelperina, S.E., Skidan, I.N., Antropov, A.S., Kivman, G.Y., Kreuter, J., 1999. Significant transport of doxorubicin into the brain with polysorbate 80-coated nanoparticles. Pharm. Res. 16, 1564–1569.

Hong, R.L., Tseng, Y.L., 2001. Phase I and pharmacokinetic study of a stable, polyethylene-glycolated liposomal doxorubicin in patients with solid tumors: the relation between pharmacokinetic property and toxicity. Cancer 91, 1826–1833.

Hughes, C.S., Vaden, S.L., Manaugh, C.A., Price, G.S., Hudson, L.C., 1998. Modulation of doxorubicin concentration by cyclosporin A in brain and testicular barrier tissues expressing P-glycoprotein in rats. J. Neurooncol. 37, 45–54.

Huwyler, J., Wu, D., Pardridge, W.M., 1996. Brain drug delivery of small molecules using immunoliposomes. Proc. Natl. Acad. Sci. U.S.A. 93, 14164–14169.

Lachatre, F., Marquet, P., Ragot, S., Gaulier, J.M., Cardot, P., Dupuy, J.L., 2000. Simultaneous determination of four anthracyclines and three metabolites in human serum by liquid chromatography–electrospray mass spectrometry. J. Chromatogr. B 738, 281–291.

Langer, F., Wintzer, H.O., Werner, M., Weber, C., Brummendorf, T.H., Bokemeyer, C., 2006. A case of pulmonary carcinosarcoma (squamous cell carcinoma and osteosarcoma) treated with cisplatin and doxorubicin. Anticancer Res. 26, 3893–3897.

Lind, P.A., Naucler, G., Holm, A., Gubanski, M., Svensson, C., 2007. Efficacy of pegylated liposomal doxorubicin in patients with advanced hepatocellular carcinoma. Acta Oncol. 46, 230–233.

Lundberg, B.B., Griffiths, G., Hansen, H.J., 2007. Cellular association and cytotoxicity of doxorubicin-loaded immunoliposomes targeted via Fab' fragments of an anti-CD74 antibody. Drug Deliv. 14, 171–175.

Neuwelt, E.A., Pagel, M., Barnett, P., Glassberg, M., Frenkel, E.P., 1981. Pharmacology and toxicity of intracarotid adriamycin administration following osmotic blood–brain barrier modification. Cancer Res. 41, 4466–4470.

Ohnishi, T., Tamai, I., Sakanaka, K., Sakata, A., Yamashima, T., Yamashita, J., Tsuji, A., 1995. In vivo and in vitro evidence for ATP-dependency of P-glycoprotein-mediated efflux of doxorubicin at the blood–brain barrier. Biochem. Pharmacol. 49, 1541–1544.

Rousselle, C., Clair, P., Lefauconnier, J.M., Kaczorek, M., Scherrmann, J.M., Temsamani, J., 2000. New advances in the transport of doxorubicin through the blood–brain barrier by a peptide vector-mediated strategy. Mol. Pharmacol. 57, 679–686.

Saito, T., Zhang, Z.J., Tokuriki, M., Ohtsubo, T., Shibamori, Y., Yamamoto, T., Saito, H., 2001. Cyclosporin A inhibits the extrusion pump function of p-glycoprotein in the inner ear of mice treated with vinblastine and doxorubicin. Brain Res. 901, 265–270.

Schwarzbach, M.H., Eisold, S., Burguete, T., Willeke, F., Klein-Bauernschmitt, P., Schlehofer, J.R., Herfarth, C., Ridder, R., von Knebel Doeberitz, M., 2002. Sensitization of sarcoma cells to doxorubicin treatment by concomitant wild-type adeno-associated virus type 2 (AAV-2) infection. Int. J. Oncol. 20, 1211–1218.

Sharma, U.S., Sharma, A., Chau, R.I., Straubinger, R.M., 1997. Liposome-mediated therapy of intracranial brain tumors in a rat model. Pharm. Res. 14, 992–998.

Smylie, M.G., Wong, R., Mihalcioiu, C., Lee, C., Pouliot, J.F., 2007. A phase II, open label, monotherapy study of liposomal doxorubicin in patients with metastatic malignant melanoma. Invest. New Drugs 25, 155–159.

Wang, J.C., Liu, X.Y., Lu, W.L., Chang, A., Zhang, Q., Goh, B.C., Lee, H.S., 2006. Pharmacokinetics of intravenously administered stealth liposomal doxorubicin modulated with verapamil in rats. Eur. J. Pharm. Biopharm. 62, 44–51.

Zhao, Y.L., Du, J., Kanazawa, H., Sugawara, A., Takagi, K., Kitaichi, K., Tatsumi, Y., Takagi, K., Hasegawa, T., 2002. Effect of endotoxin on doxorubicin transport across blood–brain barrier and P-glycoprotein function in mice. Eur. J. Pharmacol. 445, 115–123.